Large internal waves advection in very weakly stratified deep Mediterranean waters

Hans van Haren[1] and Louis Gostiaux[2]

Received 16 September 2011; revised 25 October 2011; accepted 25 October 2011; published 29 November 2011.

[1] The Eastern Mediterranean Sea contains relatively small trenches O(1–10 km) horizontal width that go deeper than 4000 m. At a first glance, these deep waters are homogeneous, with weak currents <0.1 m s^{-1}. This viewpoint is modified after evaluation of new detailed yearlong temperature observations using 103 high-precision sensors that reveal intense variability of internal waves. Even though temperature variations are within the range of a few mK only, requiring precise correction for the adiabatic lapse rate during post-processing, the images are permanently dynamic. The weak density stratification of buoyancy close to the inertial frequency supports large turbulent overturns indirectly governed or advected by large internal waves. In strongly stratified (near-surface) waters low-frequency inertial internal motions are horizontal, but here they attain a vertical current amplitude sometimes comparable to horizontal currents. This results in occasionally very large internal wave amplitudes (250 m peak-trough), which are generated via geostrophic adjustment presumably from local collapse of fronts. **Citation:** van Haren, H., and L. Gostiaux (2011), Large internal waves advection in very weakly stratified deep Mediterranean waters, *Geophys. Res. Lett.*, *38*, L22603, doi:10.1029/2011GL049707.

1. Introduction

[2] The deep-sea is generally considered a dark and motionless environment, with little life excitement. Although absolute numbers of marine biology species and their abundance are indeed gradually declining with depth [*Vinogradov*, 1961; *Priede et al.*, 2008], the sparsely filled environment is not a void. In comparison with the deep ocean, e.g., in parts of the North-Atlantic, faunal groups are less abundant by a factor of about 10 in the deep Mediterranean at comparable depths [*Priede et al.*, 2008]. The same authors demonstrate that in the Mediterranean itself a factor of 10 variability in abundance is found at any given depth between different basins, with the lower values found in the eastern basin around Greece.

[3] From a physics point of view, the dynamics of water motions seem to become weaker the further one gets from surface forcing by winds and waves and as the static stability in terms of vertical density gradient ('stratification') diminishes. This stability, common in the ocean with warm water above cold and fresh water less dense than salty, supports small- to meso-scale motions in the interior in the form of internal waves. As with the biology, little of the details is known about the physics of the deep-sea. Some aspects of deep-ocean flow structures have been revealed in the past [*Armi and D'Asaro*, 1980; *Thorpe*, 1987]. As will be demonstrated using high-resolution modern electronics instrumentation, foremost temperature (T) sensors and some additional current meters, dynamics do not come to a halt below, say, 3000 m. In fact, the motion in the deep-sea is observed to be as dynamic as that near the sea-surface, with permanently varying internal wave motions and turbulent instabilities.

[4] In the deep Mediterranean motions are dominated in two frequency (σ) bands: inertial ($\sigma \approx$ f) and mesoscale subinertial ($\sigma \ll$ f), whilst tides are weaker. The inertial frequency $f = 2\Omega\sin\varphi$ is the vertical Coriolis parameter of the Earth rotational vector $\mathbf{\Omega}$ at latitude φ; in the Ionian Sea, where the present observations are made, the local inertial period is 20.06 hours.

[5] Geostrophic adjustment leads to the generation of inertial motions, either locally as transients associated with collapse of horizontal density gradients ('fronts') thereby generating baroclinic instabilities [*Rhines*, 1988; *Tandon and Garrett*, 1994; *Boccaletti et al.*, 2007], or from downward propagating free internal waves by passages of atmospheric disturbances [*Gill*, 1982]. Under well-stratified conditions, horizontal inertial motions are circular with virtually no vertical excursions of density interfaces ($\eta \approx 0$). Their vertical length scales are small O(10 m) so that they dominate vertical shear across the stratification. Under weakly stratified conditions, when buoyancy frequency N = O(f), they describe circles that are tilted with respect to the axis of Earth rotation and whose projection on the horizontal plane describe ellipses [*van Haren and Millot*, 2004] so that vertical motions (w) no longer vanish at f but can be of the same order of magnitude as horizontal ones [*van Haren and Millot*, 2005].

[6] Here we present detailed vertical excursions at f and other internal wave frequencies, which can attain 100's of meters in the weakly stratified deep Eastern Mediterranean. These excursions are not a one-time observation, but rather omnipresent in a yearlong record.

2. Materials and Methods

[7] A 3300 m long mooring with self-contained instruments was placed in the Ionian Sea at 36° 37.657′ N, 21° 24.907′ E, water depth H = 4450 m, from December 2009 to February 2011. The site is a potential location for the future cubic kilometer Neutrino Telescope ('KM3NeT'). It is nearly flat, but it is surrounded by relatively steep topography (Figure 1a). The mooring consists of several Nortek Aqua-Dopp 2 MHz acoustic current meters distributed over the line

[1]Royal Netherlands Institute for Sea Research, Den Burg, Netherlands.
[2]CNRS/Grenoble-INP/UJF-Grenoble 1, LEGI UMR 5519, Grenoble, France.

0094-8276/11/2011GL049707

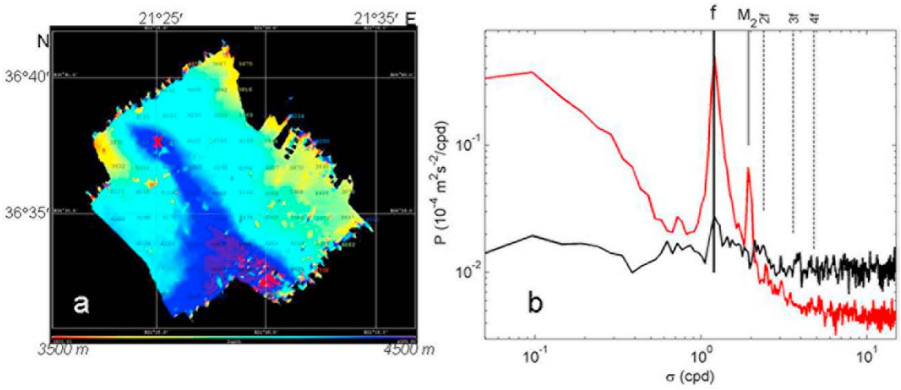

Figure 1. (a) Shipboard multibeam image obtained just prior to mooring launch (x) in northern part of trench. Colour coding for 3500 (red) to 4500 m (blue); red speckles near the bottom are errors. (b) Kinetic energy (red) and vertical current (black) spectra. Several frequencies are indicated: inertial frequency (f) including several higher harmonics and semidiurnal lunar tidal (M_2).

(of which two are at 3975, 4275 m) and 103 independent NIOZ4 T-sensors between 3977 and 4079 m at 1.0 m intervals. The current meters sample every 900 s, the synchronized T-sensors every 1 s. The standard deviation of individual current estimates is 0.01 m s^{-1} for [u, v] and 0.015 m s^{-1} for w, which reduces by a factor of about 9 for inertial period motions. The 1-m interval mounting of T-sensors proved adequate and was little disturbed by non-physical conditions such as mooring motions. Pressure (p) variations (<0.1 dBar; $\Delta z \sim$<0.1 m) due to mooring drag were equivalent to the p-sensors' noise level, over the entire yearlong period. Maximum horizontal current speeds were 0.08 m s^{-1} at the level of the T-sensors. These motions were dominated at sub-inertial and inertial frequencies (Figure 1b).

[8] NIOZ4 T-sensors are an update of NIOZ3 [*van Haren et al.*, 2009]. They have similar specifications: noise, and in this set-up digitization, levels of 6×10^{-5}°C (60 μK), precision $<1 \times 10^{-3}$°C, potential endurance 1.5 years when running at 1 Hz. As the deep Mediterranean is known for its very small temperature variations, the present exercise was the most challenging for NIOZ T-sensors so far. Extensive calibration and data inspection revealed a slow drift ($\sim$1 mK/mo) of the new, un-aged sensors. It was corrected during post-processing. Some problems with energy consumption and data file closure resulted in 19 sensors delivering inadequate data; these have been interpolated between neighboring sensors.

[9] The large number of T-sensors is potentially sufficient to compute vertical excursions (η) of temperature (density) interfaces. Contributions to density variations $\delta\rho = -\alpha\delta\Theta + \beta\delta S$, α and β heat and salt expansion coefficients, respectively, of absolute salinity (S) and conservative temperature (Θ; replacing, although dynamically equivalent to, potential temperature) [*McDougall et al.*, 2009] (see also TEOS, http://www.teos-10.org/) can vary independently. Here, their relationship is reasonably tight, they virtually compensate each other despite large (z, t)-variations (Figure 2) so that the density ratio $R = |\alpha\delta\Theta/\beta\delta S| = 0.8 \pm 0.4$ and conservative temperature can roughly act as tracer for density variations although inversions are commonly seen in smoothed density profiles (Figure 2a) and Θ (Figure 2c). However, as the vertical density stratification is extremely weak resulting in buoyancy frequency $0 < N < 4f$, with a mean $N \approx f$, based on CTD-profiles (Figure 2a), isotherm displacements representing η easily exceed the 102-m T-range. Current meter data above and below the T-sensors are used to independently compute a T-range-mean $\eta(t)$ from the linear (wave) relationship,

$$\eta(t) = \int w dt, \tag{1}$$

assuming, due to lack of observational evidence, advection is small for large-scale internal waves. As will be demonstrated below, this assumption is reasonable following comparison of the estimates (1) using current meter data with isotherm displacements observed using the thermistor string array. The w-data and thus η are smoothed to twice per hour using a running mean, in contrast with the 1-Hz T-sensor sampling.

3. Observations

[10] Over a vertical range of 500 m containing that of the T-sensors, 14 hour shipborne CTD-yoyo shows T, S variations that exceed CTD-sensors' noise (Figure 2). Directly observed T increases with depth which is mainly attributable to pressure effects, as it slopes like the local adiabatic lapse rate $\Gamma = 1.86876 \times 10^{-4}$ °C m^{-1} (green line in Figure 2d). Γ is removed from moored T-data during post-processing, $\Delta T = T - T_0 - \Gamma(z - z_0)$, $T_0(z_0)$ temperature at $z_0 = 4026$ m, being a rough Θ-estimate, to obtain images relevant for dynamics.

[11] Resulting corrected relative ΔT-image has a typical range of $\pm$0.001°C (1 mK), within which all meso-, inertial- and small-scale variability occurs, to within the 1-m observational resolution (Figure 3). This vertical resolution is much smaller than the Ozmidov scale of largest turbulent overturn $L_O = (\varepsilon/N^3)^{1/2} \approx 28$ m for data estimated at the end of this Section, but much larger than the Kolmogorov scale of turbulence dissipation $L_K = (\nu^3/\varepsilon)^{1/4} \approx 0.01$ m, where ν denotes the kinematic viscosity. The ΔT-variability is a physical signal that extends above noise level. Coherent motions are observed well-exceeding the distance of 1 m between individual sensors. Large-scale structures are seen to exceed the entire 102-m range of thermistors, apparently

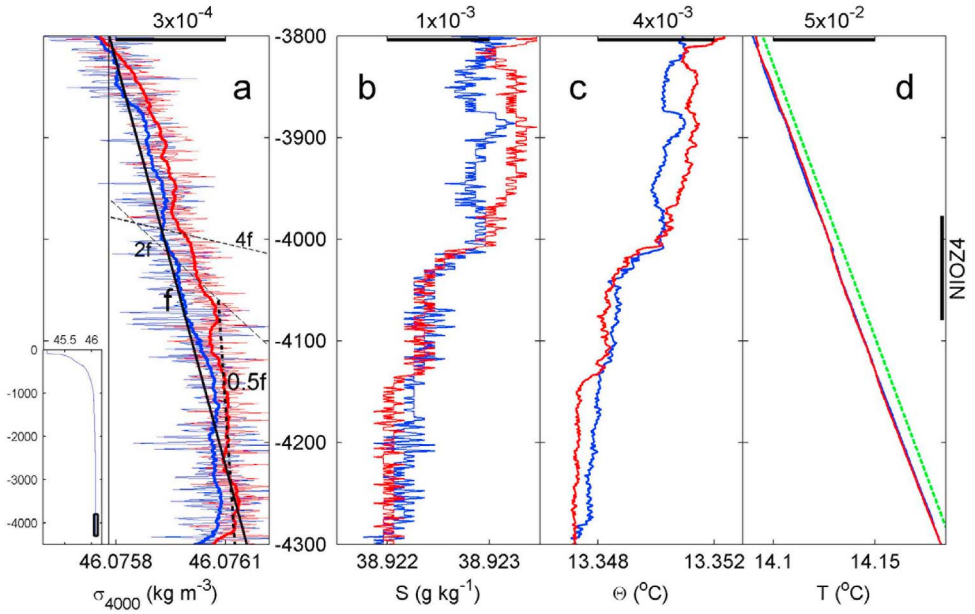

Figure 2. Shipborne yoyo-CTD observations near the mooring on a single day (29/01/2011), showing 2 (out of 19) deep profiles obtained 5 hours apart, with the ship stationary to within ±10 m. (a) Density anomaly, referenced to 4000 m, with several slopes indicated demonstrating the extremely weak density stratification $N \approx f$ ($z < -4100$ m) and $N = 0.5f$ ($-4100 < z < -4300$ m) on large vertical scales, and $0 < N < 4f$ in layers of thickness $\ll 100$ m. The thin color profiles are 1-m binned data (standard error $\approx 2 \times 10^{-4}$ kg m^{-3}), the thick color profiles their 30-m running means (standard error $\approx 3 \times 10^{-5}$ kg m^{-3}). The entire vertical profile is seen in the inset. (b) Absolute salinity (TEOS, http://www.teos-10.org/) (1-m binned standard error $\approx 2 \times 10^{-4}$ g kg^{-1}). (c) Conservative temperature (http://www.teos-10.org/) (1-m binned standard error $\approx 2 \times 10^{-4}$ °C). (d) Observed temperature, with depth-range of moored T-sensors indicated. The green dashed profile has the slope of local adiabatic lapse rate (Γ).

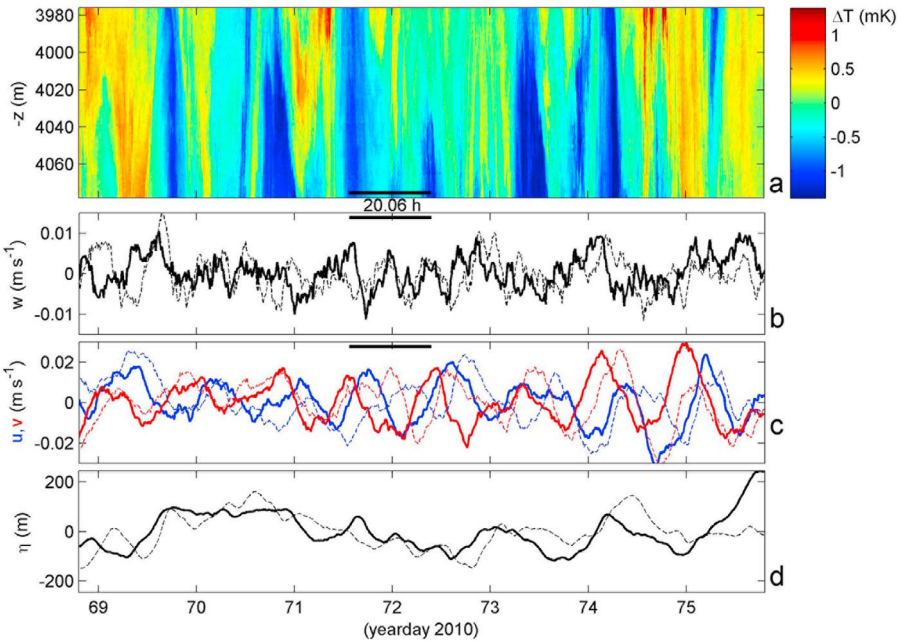

Figure 3. One week of deep internal wave observations. (a) Depth-temperature image relative to Γ. The inertial period is indicated. (b) Two-hourly smoothed vertical currents observed 2 m above uppermost T-sensor (solid) and 196 m below lowest (dashed). (c) Corresponding horizontal current components u (blue) and v (red). Note the scale increase compared to Figure 3b by a factor of 2. (d) Vertical excursions computed using (1) with w taken from Figure 3b.

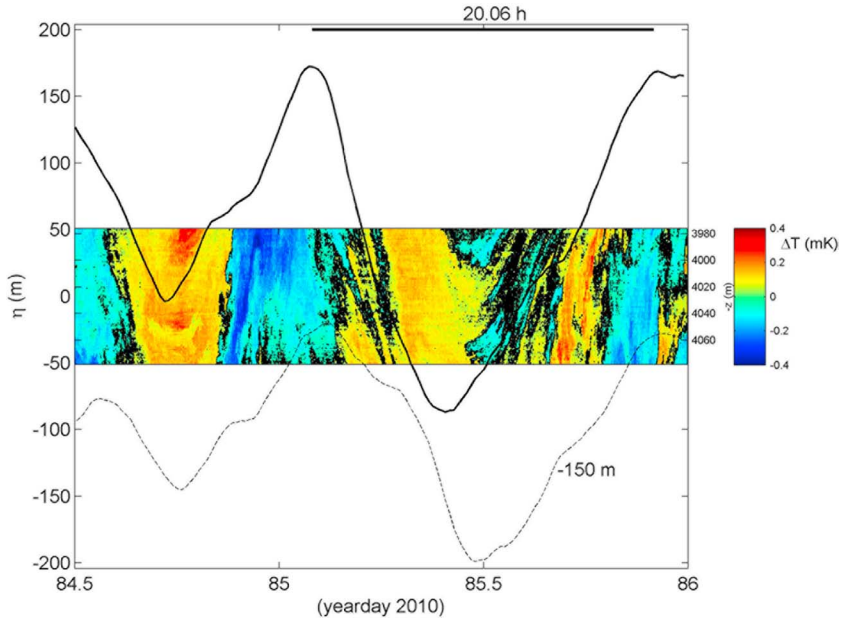

Figure 4. One-and-a-half day composite of vertical excursions computed using vertical current data in (1) and 10-s smoothed T-observations relative to Γ (note the total range of 800 μK). The upper current meter excursion is around its mean depth; that of the lower should be displaced 150 m deeper. Largely, the computed excursions match those of the detailed ΔT-observations, of which (arbitrarily chosen) ΔT = 0 is indicated (black).

vertically coherent, but more often demonstrating small vertical phase shifts. This suggests wave propagation. As the dominant horizontal currents are inertial motions (20.06 h), frontal passages are easily excluded.

[12] Wave propagation is further evidenced as the depth-time ΔT-image (Figure 3a) also shows quasi-coherent structures at frequencies smaller than inertial, with periods of a few hours (e.g., day 73). These are also seen in vertical currents above and below the thermistors (Figure 3b). Small waves have amplitudes of $|w| \approx 0.2 \times 10^{-2}$ m s^{-1}, but $|w_f| = 0.5 - 1 \times 10^{-2}$ m s^{-1}, which is not small considering the observed horizontal inertial particle speeds of $1 - 3 \times 10^{-2}$ m s^{-1} (Figure 3c). Inertial wave propagation may also be inferred from the latter observations, considering the phase differences between u (or v) at depths 300 m apart. High-frequency motions are less dominant in [u, v] than in w, as is common for wave motions near $N \sim 3 - 4f$ (estimate for this example). Integration following (1) low-pass filters w, resulting in slow inertial and sub-inertial η = 100-200 m typically (Figure 3d). Although measured at single depths, they reasonably represent large-scale [inertial] internal wave excursions, following the significantly coherent records 300 m apart. Observed downward phase differences are found also at sub-inertial frequencies, like in the detailed T-sensor data. Observations showing opposite motions or excursions (π-phase difference) are commonly accompanied by static instabilities, e.g., days 71.0, 73.2, 74.0, 74.5. Isopycnal excursions including layers of varying temperature suggest small-scale density compensation following lateral or slanted instabilities, e.g., days 69.5, 70.0, 70.5, 75.0, which can attain the form of vigorous near-vertical convective overturning.

[13] In a particular, arbitrary, 36 hours zoom (Figure 4), further details are seen within the large-scale inertial waves, all (just) within technical limits of the instrumentation. In this extremely weak ΔT-variation (totaling 8×10^{-4} °C only), the aspect ratio equals 1, horizontal near-inertial motions describe an elliptic path, $|w_f| \leq\leq 2.5 \times 10^{-2}$ m s^{-1} and large η = 250 m (peak-trough). This η is nearly twice the largest non-linear internal wave excursion observed so far in the ocean [*Liu et al.*, 2006].

[14] Such w- and ΔT-variations are also observed at smaller scales, which remain similarly coherent over depth-time. Occasionally however, internal waves start overturning and apparent static convective (T-only) instabilities, still coherent over appreciable scales, dominate (e.g., day 85). Most evidence of turbulent convection is observed in the form of presumably slanted layers of alternating relatively cold/fresh and warm/salty water that partially compensate each other in density variations (R ≈ 1): (remnants of) convective plumes [*Sheremet*, 2004; *van Haren and Millot*, 2009]. These are ubiquitous in the images, e.g., days 84.9, 85.2, 85.5-86.0, implying a rapid turbulence process, of which we have resolved scales between 2 and 102 m in the vertical. This apparent vigorous overturning in the ΔT-image (Figure 4) and the regular overturns observed in density variations by CTD (Figure 2a) suggest that not all of convection is compensated, even though some of it may be (compare Figures 2b and 2c). Crudely quantifying this as mixing using overturning scales [*Thorpe*, 1987], based on ΔT-observations alone, results in a 1.5 days (Figure 4) depth-mean eddy diffusivity $K_z = 10^{-2}$ m^2 s^{-1} and turbulence dissipation rate $\varepsilon = 2 \times 10^{-10}$ W kg^{-1}, against $N = 4.5 \times 10^{-5}$ s^{-1} = 0.53f computed from reordered local ΔT for this 1.5 day period. As near-inertial motions are the dominant internal waves, the vertically slanting convection layers are observed with same periodicity. It remains to be established whether the inertial motions actually drive this convection. Topography may not be important, as similar observations

have been made above open, relatively flat plains east of Sicily (not shown).

4. Discussion

[15] Like in the Western Mediterranean, this deep Ionian Sea is characterized by extremely weak stratification which is in permanent motion. The dominant motion is around the inertial frequency, mainly as freely propagating internal waves. Large vertical scales of such waves are observed. Their non-negligible vertical current component is understood, as the smaller N allows these inertio-gravity waves (IGW) to become increasingly affected by the horizontal Coriolis parameter (see *Gerkema et al.* [2008] for a review).

[16] The result is, first, up- and down pumping of stratification layers and material over O(100) m ($w \approx 0.01$ m s^{-1}), every day. Second, the associated shear of the waves, which have aspect ratios of 0.1–1, will tilt, as conjectured for near-surface waters by [*Hosegood et al.*, 2008], any horizontal gradients especially those created by (vertical or planetary-slanted) convection tubes [*Straneo et al.*, 2002] to the point of marginal stability so that the gradient Richardson number (stable stratification over destabilizing shear) is smaller than one [*van Haren*, 2008]. Such planetary-slanted convection is in the direction of the earth rotation, but appears stably stratified in the direction of gravity, except at the north-pole. Third, the waves transfer energy to turbulent convection thereby generating mixing. This mixing is in already nearly-homogeneous waters, but following the observations lateral (stability) supply of varying Θ-S water mass characteristics seems to provide sufficient fresh input for restratification. The quasi-compensating deep Θ and S are similar to those observed in vigorously mixed near-surface waters [*Rudnick and Ferrari*, 1999; *Sheremet*, 2004]. Once compensated they are long-lived [*Rudnick and Ferrari*, 1999]. However, not all is compensated and the observed overturns also resemble near-surface mixed-layer instabilities [*Boccaletti et al.*, 2007]. The precise mechanism behind instabilities in the present observations needs further investigation, but coupling with internal inertial shear along lines of rotational stability [*Greenspan*, 1980] and localized breaking inertial waves [*Saint-Guily*, 1972] seem not fortuitous.

[17] The deep Mediterranean trench waters are found never quiescent or void in motions and turbulent mixing, with consequences for life abundance in such waters. It is not expected that the observed IW-turbulence are a hazard for a future neutrino telescope, when the above vertical motions are accounted for.

[18] **Acknowledgments.** We enjoyed the assistance of the crews of the R/V Pelagia and Meteor. We thank M. Laan for all the elaborate work on NIOZ-thermistors and T. Hillebrand and NIOZ-MTM for preparing and deploying the instruments. This project is supported in part by the Dutch Organization for the Advancement of Scientific Research NWO (ESFRI-roadmap; large research facilities) as the Dutch Nikhef-NIOZ-KVI contribution to KM3NeT.

[19] The Editor thanks two anonymous reviewers for their assistance in evaluating this paper.

References

Armi, L., and E. A. D'Asaro (1980), Flow structures of the benthic ocean, *J. Geophys. Res.*, *85*, 469–484, doi:10.1029/JC085iC01p00469.

Boccaletti, G., R. Ferrari, and B. Fox-Kemper (2007), Mixed layer instabilities and restratification, *J. Phys. Oceanogr.*, *37*, 2228–2250, doi:10.1175/JPO3101.1.

Gerkema, T., J. T. F. Zimmerman, L. R. M. Maas, and H. van Haren (2008), Geophysical and astrophysical fluid dynamics beyond the traditional approximation, *Rev. Geophys.*, *46*, RG2004, doi:10.1029/2006RG000220.

Gill, A. E. (1982), *Atmosphere-Ocean Dynamics*, 662 pp., Academic, Orlando, Fla.

Greenspan, H. P. (1980), *The Theory of Rotating Fluids*, 328 pp., Cambridge Univ. Press, Cambridge, U. K.

Hosegood, P. J., M. C. Gregg, and M. H. Alford (2008), Restratification of the surface mixed layer with submesoscale lateral density gradients: Diagnosing the importance of the horizontal dimension, *J. Phys. Oceanogr.*, *38*, 2438–2460, doi:10.1175/2008JPO3843.1.

Liu, C.-T., R. Pinkel, M.-K. Hsu, J. M. Klymak, H.-W. Chen, and C. Villanoy (2006), Nonlinear internal waves from Luzon Strait, *Eos Trans. AGU*, *87*, 449, doi:10.1029/2006EO420002.

McDougall, T. J., R. Feistel, F. J. Millero, D. R. Jackett, D. G. Wright, B. A. King, G. M. Marion, C.-T. A. Chen, and P. Spitzer (2009), Calculation of the thermodynamic properties of seawater: Global ship-based repeat hydrography manual, *IOCCP Rep. 14*, 131 pp., U. N. Educ., Sci. and Cult. Organ., Paris.

Priede, I. G., A. Jamieson, A. Heger, J. Craig, and A. F. Zuur (2008), The potential influence of bioluminescence from marine animals on a deep-sea underwater neutrino telescope array in the Mediterranean Sea, *Deep Sea Res., Part I*, *55*, 1474–1483, doi:10.1016/j.dsr.2008.07.001.

Rhines, P. B. (1988), Mixing and large-scale ocean dynamics, in *Small-Scale Turbulence and Mixing in the Ocean*, edited by J. C. J. Nihoul and B. M. Jamart, pp. 263–284, Elsevier, Amsterdam.

Rudnick, D. L., and R. Ferrari (1999), Compensation of horizontal temperature and salinity gradients in the ocean mixed layer, *Science*, *283*, 526–529, doi:10.1126/science.283.5401.526.

Saint-Guily, B. (1972), On the response of the ocean to impulse, *Tellus*, *24*, 344–349, doi:10.1111/j.2153-3490.1972.tb01562.x.

Sheremet, V. A. (2004), Laboratory experiments with tilted convective plumes on a centrifuge: A finite angle between the buoyancy and the axis of rotation, *J. Fluid Mech.*, *506*, 217–244, doi:10.1017/S0022112004008572.

Straneo, F., M. Kawase, and S. C. Riser (2002), Idealized models of slantwise convection in a baroclinic flow, *J. Phys. Oceanogr.*, *32*, 558–572, doi:10.1175/1520-0485(2002)032<0558:IMOSCI>2.0.CO;2.

Tandon, A., and C. Garrett (1994), Mixed layer restratification due to a horizontal density gradient, *J. Phys. Oceanogr.*, *24*, 1419–1424, doi:10.1175/1520-0485(1994)024<1419:MLRDTA>2.0.CO;2.

Thorpe, S. A. (1987), Current and temperature variability on the continental slope, *Philos. Trans. R. Soc. London, Ser. A*, *323*, 471–517, doi:10.1098/rsta.1987.0100.

van Haren, H. (2008), Abrupt transitions between gyroscopic and internal gravity waves: the mid-latitude case, *J. Fluid Mech.*, *598*, 67–80, doi:10.1017/S0022112007009524.

van Haren, H., and C. Millot (2004), Rectilinear and circular inertial motions in the western Mediterranean Sea, *Deep Sea Res., Part I*, *51*, 1441–1455, doi:10.1016/j.dsr.2004.07.009.

van Haren, H., and C. Millot (2005), Gyroscopic waves in the Mediterranean Sea, *Geophys. Res. Lett.*, *32*, L24614, doi:10.1029/2005GL023915.

van Haren, H., and C. Millot (2009), Slantwise convection: A candidate for homogenization of deep newly formed dense waters, *Geophys. Res. Lett.*, *36*, L12604, doi:10.1029/2009GL038736.

van Haren, H., M. Laan, D.-J. Buijsman, L. Gostiaux, M. G. Smit, and E. Keijzer (2009), NIOZ3: independent temperature sensors sampling yearlong data at a rate of 1 Hz, *IEEE J. Oceanic Eng.*, *34*, 315–322, doi:10.1109/JOE.2009.2021237.

Vinogradov, M. E. (1961), Feeding of the deep-sea zooplankton, *Rapp. P. V. Reun. Cons. Int. Explor. Mer*, *153*, 114–120.

L. Gostiaux, CNRS/Grenoble-INP/UJF-Grenoble 1, LEGI UMR 5519, Grenoble, F-38041, France.

H. van Haren, Royal Netherlands Institute for Sea Research, PO Box 59, NL-1790 AB Den Burg, Netherlands. (hans.van.haren@nioz.nl)